Chiral states of electromagnetic fields originated from ferrite-based microwave vortices

M. Sigalov, E. O. Kamenetskii,[a] and R. Shavit
Ben-Gurion University of the Negev, Beer Sheva 84105, Israel

(Received 28 February 2008; accepted 27 October 2008; published online 12 December 2008)

Electromagnetic vortices in a microwave cavity with an inserted piece of a magnetized ferrite appear due to the time-reversal symmetry breaking effect. We reveal numerically that the Poynting-vector vortices are possible in open resonant microwave structures with ferrite inclusions. We demonstrate a pair of resonances which have opposite vortex rotations at the same direction of time given by the direction of the magnetization precession. There are two coalescent resonances with different chirality. We show that the structures of the radiating near and far fields are intimately related to the ferrite-induced topological singularities. The observed far-field polarization structures represent a doublet of chiral vortices in space originated from a doublet of resonant chiral states in a patch resonator with an enclosed ferrite disk. © *2008 American Institute of Physics*.
[DOI: 10.1063/1.3040008]

I. INTRODUCTION

Vortices can be easily observed in water. They are a common occurrence in plasma science. In recent years, there has been a considerable interest in vortices of electromagnetic fields. There are electromagnetic processes with broken symmetry characterized by different topological effects. Study of vortices with optical phase singularities has opened up a new frontier in optics.[1] In microwaves, there is a special interest in electromagnetic vortices created by ferrite particles with the ferromagnetic resonance (FMR) conditions.

A ferrite is a magnetic dielectric with low losses. This may allow for electromagnetic waves to penetrate the ferrite and results in an effective interaction between the electromagnetic waves and the magnetization within the ferrite. Such an interaction can demonstrate very interesting physical features. Due to the nonzero purely imaginary off-diagonal component of the permeability tensor in the proximity of the FMR, the phase of the wave reflected from the ferrite-dielectric interface depends on the direction of the incident wave.[2] This time-reversal symmetry (TRS) breaking effect is the cause why in a resonant structure with an enclosed ferrite sample the electromagnetic-field eigenfunctions are complex, even in the absence of dissipative losses. This means that fields of eigenoscillations are not the fields of standing waves in spite of the fact that eigenfrequencies of a cavity with a ferrite sample are real.[3] An insertion of a piece of a magnetized ferrite into the resonator domain causes a microwave resonator to behave under odd TRS. In this case a ferrite sample may act as a topological defect causing induced electromagnetic vortices. Based on numerical simulation described in Ref. 4 it has been shown that the power-flow lines of the microwave-cavity field interacting with the ferrite sample in the proximity of its FMR form whirlpool-like electromagnetic vortices. We found that in such nonintegrable structures, magnetic gyrotropy and geometrical factors lead to the effect of symmetry breaking resulting in effective chiral magnetic currents and topological magnetic charges.[5,6]

One of the main features of microwave vortices shown in Refs. 4–6 is the fact that such "swirling entities" appear only when a ferrite sample is placed in a resonant system. While our previous numerical experiments with ferrite-based vortices were aimed to analyze the microwave fields in closed resonant systems (cavities) with low losses, studies of ferrite-based vortices in open microwave resonators could also be a very attractive problem. In this paper we find that in such resonant structures one can observe pairs of coalescent resonance modes. Recent experiments[7] demonstrate the effects of lifting the degeneracy of resonances in a microwave resonator with an enclosed ferrite sample. On the other hand, the two-energy-level resonant system exhibiting different chiralities is known from experimental studies of a dissipative microwave resonator with a special topological structure.[8] In the present numerical studies we show that the observed pairs of resonances in open resonant systems with ferrite samples have different directions of the Poynting-vector vortex rotation at the same direction of time. There are, in fact, the coalescent resonant states with different chirality.

Open resonators are radiating systems. A special interest in our problem concerns possible correlation of the electromagnetic vortex phase singularities and chiral states with the near-field and far-field properties of the electromagnetic fields radiating from open resonant structures with enclosed ferrites. Regarding this aspect, it is relevant to note an interesting phenomenon of relationships between the vortex-type phase singularities and the far-field radiation pattern which has been shown recently in a slit-metal-plate structure.[9] On the other hand, in Ref. 10 the authors observed handedness-sensitive rotations of the far-field polarization states for visible light diffracted from an artificial planar-chirality medium. These experimental results unambiguously show that polarization changes in light diffracted from a chiral struc-

[a]Electronic mail: kmntsk@ee.bgu.ac.il.

ture demonstrate a true signature of the medium chirality. Theoretical studies of this effect are represented in Ref. 11.

Here we show that the Poynting-vector phase singularities and the electromagnetic chiral states of the microwave resonator with ferrite-based vortices are intimately connected with the near-field structure and the far-field pattern of the electromagnetic fields. For present investigations, we use a radiating patch resonator with an enclosed small ferrite disk. Since the nonintegrable nature of the problem precludes exact analytical results for the eigenvalues and eigenfunctions, numerical approaches are required. The analysis is made with use of the HFSS (the software based on FEM method produced by ANSOFT Co.) Computer-aided design simulation programs for three-dimensional numerical modeling of Maxwell equations. In our numerical experiments, both the modulus and the phase of the fields are determined.

II. MAGNETIC GYROTROPY AND CHIRALITY

The effects of chirality shown in this paper are intimately connected with magnetic gyrotropy properties of a ferrite. The question of magnetic gyrotropy and chirality appears as a fundamental problem in electromagnetism concerning relationships between the TRS breaking and parity nonconservation properties. Our studies should be started with a brief analysis of this important question.

The electron spins within a magnetized ferrite precess with their Larmor frequency about the static magnetic field and magnetic gyrotropy is observed due to the magnetization precession dynamics. This is the TRS breaking phenomenon which is described by the Landau-Lifshitz equation $\frac{\partial \vec{m}}{\partial t} = -\gamma \vec{m} \times \vec{H}$, where $\vec{m}$ is the magnetization, $\vec{H}$ is the magnetic field, and γ is the gyromagnetic ratio. In the continual representation, one has *eigenoscillations* of magnetization for a saturated ferrite. This eigenprocess is characterized by the *right-hand* direction of the magnetization precession. For a saturated ferrite, the rf magnetization is caused only by transversal (with respect to a direction of a bias dc magnetic field) components of the rf magnetic field. The magnetic susceptibility tensor $\overleftrightarrow{\chi}$ becomes nonsymmetrical with antisymmetric off-diagonal components $i\chi_a$ and $-i\chi_a$. This property of a ferromagnetic medium is called *magnetic gyrotropy*. In materials with magnetic gyrotropy, one has a local constitutive relation: $\vec{B} = \overleftrightarrow{\mu} \cdot \vec{H}$, where $\overleftrightarrow{\mu} \equiv 1 + 4\pi \overleftrightarrow{\chi}$ (Ref. 3). The permeability tensor is transposed if the dc magnetic field is reversed. This can be regarded as the TRS breaking phenomenon. Due to magnetic gyrotropy, for plane electromagnetic waves propagating in a ferrite medium one has such effects as the Faraday rotation and birefringence. In microwaves, a ferrite is usually described by the scalar electric susceptibility. So no electric gyrotropy is assumed in such a phenomenon characterization.

Another possibility to obtain the electromagnetic field rotation is due to the so-called effects of *chirality*. In natural crystals, chirality (or optical activity) takes place because of spatial dispersion.[12,13] The signs of the antisymmetric components of the electric susceptibility are reversed when a wave vector of a propagating wave changes from $\vec{k}$ to $-\vec{k}$. Recently, some artificial chiral materials with nonlocal structural elements have been suggested for microwave[14] and optical[10,11] applications. In fact, there are composites with nonlocal structural elements.[15,16] The electromagnetic properties of chiral materials are different from materials with magnetic gyrotropy. For a plane wave propagating in a homogeneous chiral medium, one has a constitutive relation:[12,13] $\vec{D} = \varepsilon \vec{E} + i\vec{G} \times \vec{E}$, where $\vec{G}$ is the gyration vector which is parallel to the wave vector $\vec{k}$. The gyration vector is a time-even pseudoscalar observable. One can rewrite the constitutive relation for a chiral medium as $\vec{D} = \overleftrightarrow{\varepsilon}_{\text{eff}} \vec{E}$, where $\overleftrightarrow{\varepsilon}_{\text{eff}} \equiv \varepsilon + i\overleftrightarrow{G}$ is the effective permeability tensor and $\overleftrightarrow{G}$ is an antisymmetrical tensor. It is evident that for components of the tensor $\overleftrightarrow{\varepsilon}_{\text{eff}}$ in a lossless medium one has $(\varepsilon_{\text{eff}})_{ij}(\vec{k}) = (\varepsilon_{\text{eff}})^*_{ji}(-\vec{k})$.

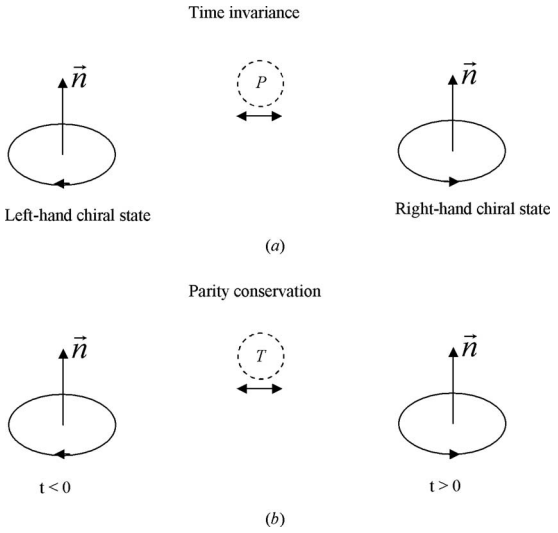

FIG. 1. Arbitrary cyclic processes illustrating difference between chirality and magnetic gyrotropy: (a) chirality; (b) magnetic gyrotropy. *P* means parity transformation and *T* means time reversal.

The hallmark of chirality is that it is exhibited by systems existing in two distinct enantiometric states that are time-invariant and interconverted by space inversion.[17] In general, it can be assumed that the effect of chirality has no evident correlation with magnetic gyrotropy. To illustrate this statement let us consider arbitrary cyclic processes in space shown in Fig. 1. In a case of chirality one has time-invariant states with the parity nonconservation [see Fig. 1(a)], but in a case of magnetic gyrotropy one has the parity conservation with the TRS breaking [see Fig. 1(b)]. This allows making the following important conclusion: to be able to discriminate between the states with different chirality in dynamical systems one should be able to realize a situation with a concrete direction of time. The cyclic processes in Fig. 1 may represent, in particular, the Poynting-vector vortices. In Ref. 4 it has been shown that in a ferrite-originated vortex, the direction of the Poynting-vector rotation changes when the dc magnetic field is reversed. This is the case of the TRS breaking shown in Fig. 1(b). In this paper we show that in a ferrite-originated vortex one can also observe the time-invariant Poynting-vector chiral states corresponding to the case of Fig. 1(a). For these chiral states, a certain direction of time is given by the direction of magnetization precession.

III. TIME REVERSAL SYMMETRY BREAKING AND TOPOLOGICAL RESONANT STATES IN RESONATORS WITH FERRITE SAMPLES

If the conjugate states $\{t\}$ and $\{-t\}$ are macroscopically distinctive, the TRS (T symmetry) is broken. In dynamical processes, there can be implications of the combined time-reversal and spatial symmetries. Combination of the time-reversal and spatial symmetries determines the properties of reciprocity and transmission of electromagnetic waves.[18]

A ferrite destroys rotational symmetry. For a microwave resonator with an enclosed ferrite sample, the fact that the resonant fields are not the fields of standing waves[3] may give very specific topological-phase characteristics. The approach using a random superposition of plane waves may give a good qualitative picture for such topological effects. A special character of the Poynting-vector distribution in a resonant system with a small ferrite sample appears due to the frequency dependence of the electromagnetic ray trajectories from a combination of three parameters: a bias magnetic field, frequency, and geometry. When a ferrite sample is placed in a certain waveguide structure, the points on the ferrite-dielectric interfaces become the symmetry breaking places. For the TE (or TM) propagating electromagnetic modes, one may use an interpretation which allows viewing the modes as pairs of two bouncing electromagnetic plane waves. This interpretation clearly shows that for a structure with an enclosed magnetized ferrite sample given, for example, in Fig. 2 there can be no identity between the rays $1\rightarrow F\rightarrow 1'$ and $1\leftarrow F\leftarrow 1'$ in the sense that these rays can acquire different phases when are reflected by the ferrite.[6,19] The refraction angle for the ray inside the ferrite depends on the position of the ferrite-dielectric interface. Moreover, for a given bias magnetic field and different frequencies, there are different refraction angles for the rays inside the ferrite. To clarify these statements on the refraction rays inside a ferrite we should refer to the well known analysis of the plane wave propagation in an infinite ferrite medium.

Let a bias magnetic field be directed along z axis and the ferrite material is described by the permeability tensor

$$\vec{\mu} = \mu_0 \begin{bmatrix} \mu & i\mu_a & 0 \\ -i\mu_a & \mu & 0 \\ 0 & 0 & 1 \end{bmatrix}. \tag{1}$$

The wave propagation in an infinite ferrite medium is characterized by the following scalar effective permeability parameter:[3]

$$\mu_{\text{eff}}(\theta_k) = \frac{2 + \sin^2\theta_k(\mu_\perp - 1) \pm \sqrt{\sin^4\theta_k(\mu_\perp - 1)^2 + 4\cos^2\theta_k\mu_a^2/\mu^2}}{2(\sin^2\theta_k + \cos^2\theta_k/\mu)}, \tag{2}$$

where θ_k is the angle between directions of the wave vector $\vec{k}$ and the bias magnetic field $\vec{H}_0$, and

$$\mu_\perp \equiv \frac{\mu^2 - \mu_a^2}{\mu}. \tag{3}$$

Two limit cases have to be taken into account: for $\theta_k = 0$ one has $\mu_{\text{eff}} = \mu \pm \mu_a$ and for $\theta_k = \pi/2$ one has $\mu_{\text{eff}} = \mu_\perp$. In a case of negligible losses in a ferrite material, it is evident that for an arbitrary angle θ_k, $\mu_{\text{eff}}(\theta_k) > 0$ when there are positive quantities of μ_{eff} in the two limit cases: $\theta_k = 0$ and $\theta_k = \pi/2$.

For a given incident angle φ (for the wave incident from a dielectric to a ferrite), the refraction angle ψ is defined as

$$\frac{\sin\psi}{\sin\varphi} = \sqrt{\frac{\varepsilon_1}{\varepsilon_2\mu_{\text{eff}}(\theta_k)}}, \tag{4}$$

where ε_1 and ε_2 are, respectively, the dielectric and ferrite permittivity parameters. The angles ψ and θ_k are in mutual correlation. This depends on a position of a ferrite-dielectric surface. For example, in the case shown in Fig. 3(a) one has $\theta_k = \frac{\pi}{2} - \psi$, while for the case shown in Fig. 3(b) one has $\theta_k = \psi$.

A simple calculation shows that for the ferrite parameters used in our numerical experiments, one has positive quantities of real parts of parameters μ and μ_a as well as positive quantities of real parts of parameters $\mu_\perp$ and $\mu \pm \mu_a$ at these frequencies. So for negligible losses in a ferrite material one has $\mu_{\text{eff}}(\theta_k) > 0$ for any angle θ_k and, therefore, the propagating wave behavior inside a ferrite. The frequency dependence of the ray trajectories gives evidence for possible creation of resonant states with different topological structures.

The TRS breaking effect can lead to creation of the Poynting-vector vortices. In quasi-two-dimensional microwave systems with enclosed ferrite samples, in a vacuum region of the TE polarized microwave resonators (with the electric field component E_z), the time-averaged part of the Poynting vector can be written as

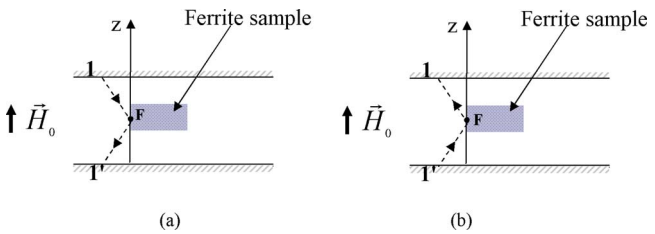

FIG. 2. (Color online) The rays in a dielectric $1\rightarrow F\rightarrow 1'$ (a) and $1\leftarrow F\leftarrow 1'$ (b) acquire different phases when are reflected by the ferrite.

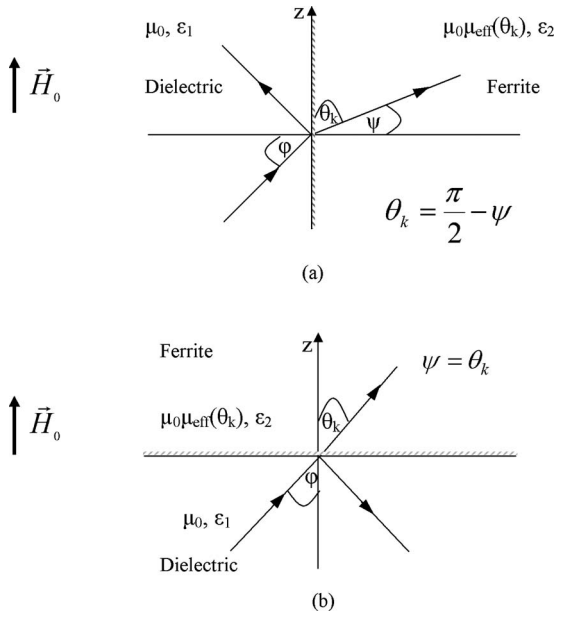

FIG. 3. Examples of two cases of relations between the angle θ_k and refraction angle ψ.

$$\vec{S} = \frac{c^2}{8\pi\omega}\mathrm{Im}(E_z^*\vec{\nabla}E_z). \tag{5}$$

and approximated by a scalar wave function.[4] The presence of a vortex means that the line integral of the spatial gradient of the phase Φ of a scalar wave function taken around the vortex center is some multiple of 2π, i.e.,

$$\oint \nabla\Phi dl = 2n\pi, \tag{6}$$

in which $n=\pm 1, \pm 2, \ldots$ This integral is proportional to what has become known as a topological charge. Such a topological charge corresponds to a phase singularity at a point where the wave amplitude is zero and hence the wave phase is undefined. There can be found a one-to-one relation of this representation with the current density

$$\vec{j} = \frac{\hbar}{m}\mathrm{Im}(\Psi^*\vec{\nabla}\Psi) \tag{7}$$

for the electron wave function Ψ in the corresponding quantum-mechanical system. The fact that vortices of the free-space Poynting vector in flat electromagnetic resonators appear as a consequence of the nontrivial topological structure makes this relevant for modeling quantum vortices.[2] In a wider point of view, a current-density-like quantity of mutual coherence was introduced in Ref. 20 as a quantity associated with a vortex state.

As it was shown in Refs. 4–6, for a closed microwave resonator with a ferrite inclusion the power flow lines may form the vortex structure not only outside, but also inside a ferrite region. Inside a ferrite, no analytical relations like Eq. (6) are possible. Nevertheless, a numerical analysis of the field structures inside a ferrite clearly shows that a center of the two-dimensional Poynting-vector vortex corresponds to the point of the phase singularity.[5,6]

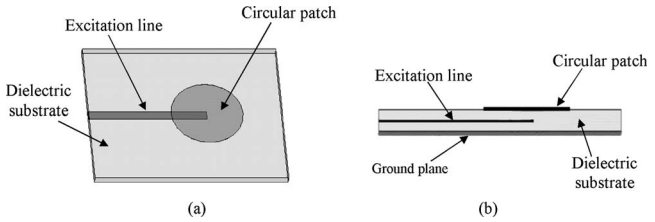

FIG. 4. A typical patch resonator excited by a microstrip line: (a) perspective view; (b) side view.

For open resonators with ferrite inclusions, two main aspects become evident in an analysis of TRS breaking properties and topological structures. The first one follows from the fact that due to the TRS breaking one may not observe single isolated resonances, but two coalescent resonances. There exists the T violating matrix element of the effective Hamiltonian which describes the coalescent resonances in a cavity with a ferrite inclusion.[7] On the other hand, the coalescence of two bound states may take place in a dissipative microwave resonator which exhibits a singularity—the so-called exceptional point—in its eigenvalue and eigenvector spectrum.[8,21] One of the key features of the coalescence is appearance of a geometric phase. In such non-Hermitian microwave cavity systems one observes distinctive chiral states as two different energy states.[8,21] The eigenfunction of the complex Hamiltonian of a two-level system at the exceptional point is expressed as

$$|\Psi\rangle \propto |1\rangle \pm i|2\rangle, \tag{8}$$

where the basis states $|1\rangle$ and $|2\rangle$ correspond to the electric field distributions of two coalescent modes of the resonator. The positive or negative sign of chirality can be defined via the direction of time. In Refs. 8 and 21 the positive direction of time was given by the decay of the eigenstates.

The above two aspects of mode coalescence in the TRS-breaking systems and mode coalescence in chiral-state dissipative resonators become very important in our consideration. As we will show, in an open resonator with a ferrite inclusion there are the eigenmode coalescence and chiral states corresponding to the Poynting-vector vortex structures.

IV. EVIDENCE FOR TWO CHIRAL STATES IN THE VORTEX FIELD STRUCTURES ORIGINATED FROM FERRITE-DISK TOPOLOGICAL DEFECTS

To study the vortex field structures originated from the ferrite-disk topological defects in an open microwave resonance system we use a patch resonator. This is a typical microwave resonator which consists of a cylindrical metal patch suspended over a ground plane. The patch is printed on a dielectric (ε_r=2.62) substrate backed by a ground plate. The patch diameter is 34 mm and the thickness of the dielectric substrate is 3.23 mm. The resonator is excited by a microstrip line through electromagnetic coupling as shown in Fig. 4. Figure 5 describes the frequency dependency of the return loss (parameter S_{11} of a scattering matrix). Figure 6 shows the fields (at a certain time phase) and the Poynting-vector distribution inside the dielectric substrate at the resonant frequency f=2.99 GHz.

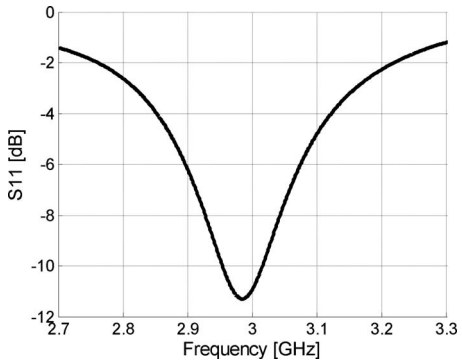

FIG. 5. A frequency characteristic of the return loss (parameter S_{11} of a scattering matrix) of a patch resonator.

To create microwave vortices we use a normally magnetized ferrite (yttrium iron garnet) disk. The disk parameters are as follows: diameter $D=8$ mm, thickness $t=1$ mm, saturation magnetization $4\pi M_s=1880$ G, $\Delta H=1$ Oe, and permittivity $\varepsilon_r=15$. The bias magnetic field is $H_0=2927$ Oe. A ferrite disk is placed in a center of a patch resonator in the gap (1.64 mm) between the feeding microstrip line and the patch. A bias magnetic field is directed along z axis. Figure 7 shows the disk position. In this position a disk is in a maximal rf magnetic field of a patch resonator. The frequency characteristic of the return loss (parameter S_{11} of a scattering matrix) of a patch resonator with an enclosed ferrite disk shown in Fig. 8 clearly demonstrates the existence of two

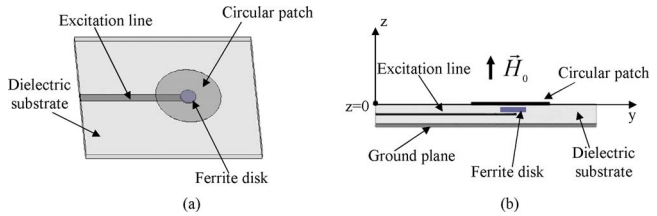

FIG. 7. (Color online) The ferrite disk position in a center of a patch resonator: (a) perspective view; (b) side view.

resonances. We will conventionally call these resonances as the upper (corresponding to the upper resonant frequency) and the lower (corresponding to the lower resonant frequency) resonances.

We start our studies of the ferrite-based vortices in a patch resonator at the frequency of the upper resonance $f=2.93$ GHz. In Fig. 9 one can observe the vortex-type Poynting vector distribution in a dielectric plate of a patch resonator corresponding to this frequency. The time dependencies of the magnetic and electric field structures inside a dielectric substrate are shown, respectively, in Figs. 10 and 11. The field vectors have a *clockwise* rotation. These field rotations result in appearance of a clockwise rotating electric dipole due to the induced electric charges on opposite sides of a cylindrical metal patch (see Fig. 11).

At the frequency corresponding to the lower resonance we obtain another picture of the vortex structure. In this case

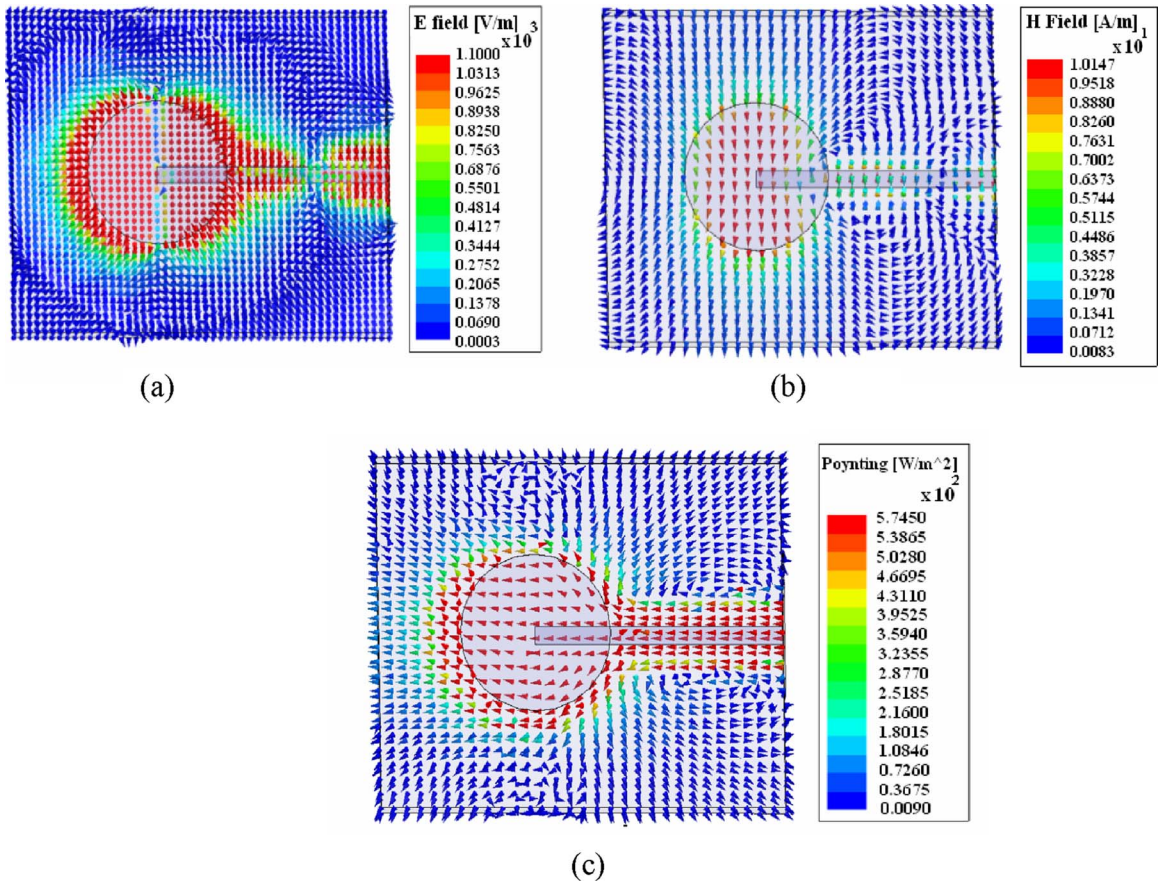

FIG. 6. (Color online) The magnetic (a) and the electric (b) field structures, and the Poynting vector distribution in a patch resonator at a resonant frequency $f=2.99$ GHz (top view).

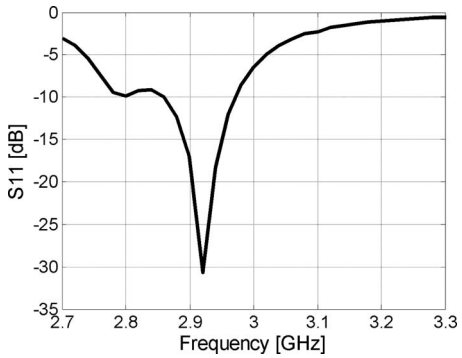

FIG. 8. A frequency characteristic of the return loss (parameter S_{11} of a scattering matrix) of a patch resonator with an enclosed ferrite disk.

the Poynting vector rotates in opposite direction with respect to the direction of the Poynting-vector rotation for the upper resonance. Figure 12 shows the vortex-type Poynting vector distribution at frequency $f=2.72$ GHz in the vicinity of the lower resonance. The cause for the Poynting vector rotation reversal becomes evident from the pictures of the time dependence of the magnetic and electric field vectors in the dielectric substrate as shown in Figs. 13 and 14, respectively. Contrary to the pictures shown in Figs. 10 and 11, at frequency $f=2.72$ GHz the magnetic and electric fields have the *counterclockwise* rotation. At this frequency the electric dipole has also the *counterclockwise* rotation. The reason why we have chosen the lower frequency $f=2.72$ GHz in the vicinity of the lower resonance, but not exactly at the frequency of the lower resonance (corresponding to frequency $f=2.8$ GHz in Fig. 8) is caused by the feature that for $f=2.72$ GHz we obtain essentially better characteristics of the circularly polarized radiated field. The fact that the frequency with the better characteristics of the circularly polarized field may not coincide exactly with the minimum of the S_{11} parameter is typical to circularly polarized antennas.[22]

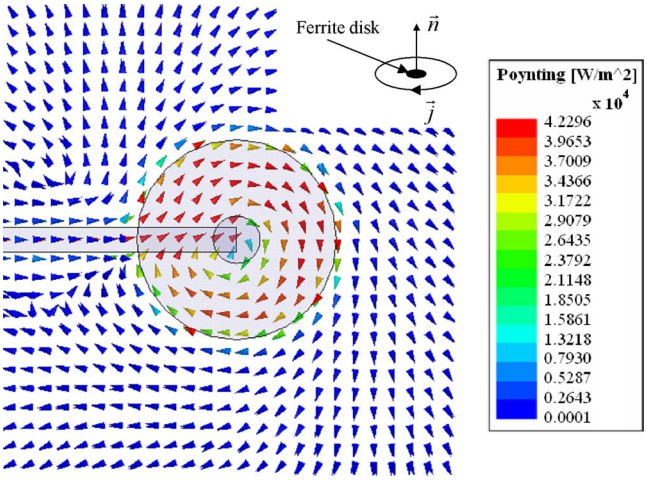

FIG. 9. (Color online) The Poynting vector distribution inside a patch resonator with a ferrite disk at the upper-resonance frequency $f=2.93$ GHz (top view). This is the left-hand chiral state. The Poynting vector can be represented as a certain current-density-like quantity $\vec{j}$, which acquires a phase of -2π after a full circle rotation. An insertion shows that a ferrite disk behaves as a topological defect with a negative topological charge.

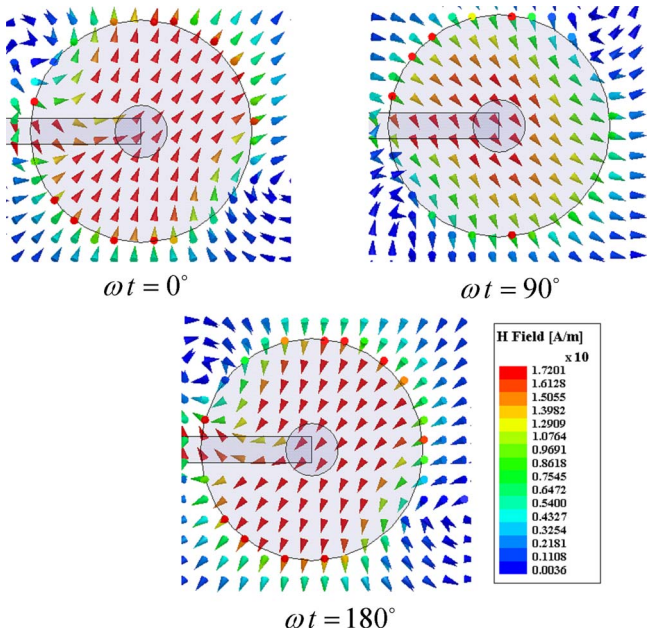

FIG. 10. (Color online) The magnetic field structure at different time phases inside a patch resonator with a ferrite disk at the upper-resonance frequency $f=2.93$ GHz (top view).

The observed field rotations in a resonator should be correlated with the direction of the magnetization precession in a ferrite. In the continual representation, one has eigenoscillations of magnetization for a saturated ferrite. This process is characterized by the *right-hand* direction of the magnetization precession.[3] As it was shown in Ref. 6, creation of the Poynting-vector vortices in a microwave cavity with a ferrite disk placed at the maximal cavity magnetic field takes place for the *left-hand* direction of the magnetic field rotation. This fact has a clear explanation. Energetically, creation

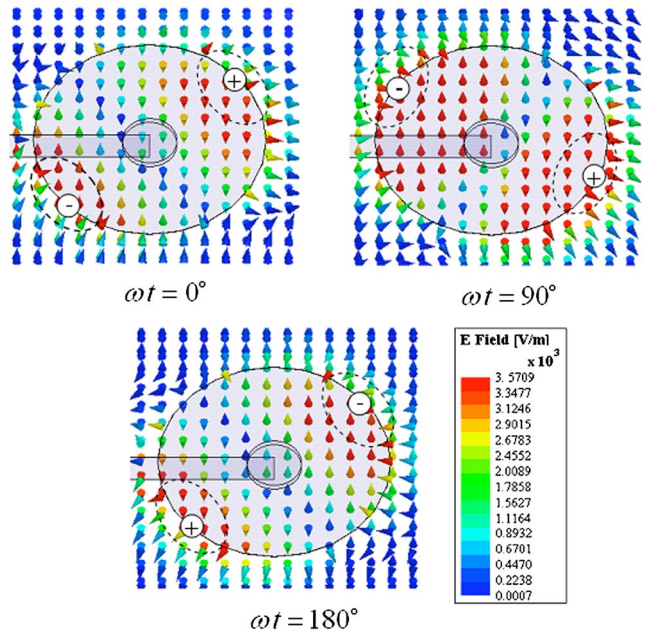

FIG. 11. (Color online) The electric field structure at different time phases inside a patch resonator with a ferrite disk at the upper-resonance frequency $f=2.93$ GHz (perspective view). There is a clockwise rotating electric dipole which appears due to electric charges on an edge of a patch.

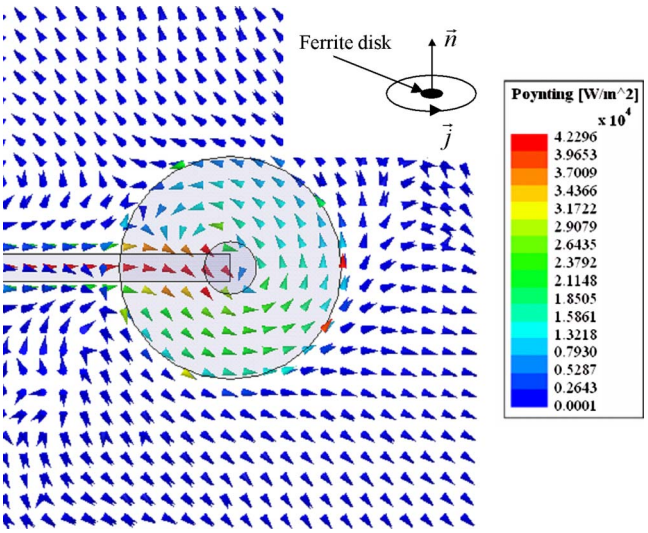

FIG. 12. (Color online) The Poynting vector distribution inside a patch resonator with a ferrite disk at the lower-resonance frequency $f=2.72$ GHz (top view). This is the right-hand chiral state. The Poynting vector can be represented as a certain current-density-like quantity $\vec{j}$, which acquires a phase of $+2\pi$ after a full circle rotation. An insertion shows that a ferrite disk behaves as a topological defect with a positive topological charge.

of the Poynting-vector vortices inside the cavity is due to the fact that there is the cavity magnetic field rotating in the opposite direction with respect to the direction of the magnetization precession. Contrary to a cavity, a patch resonator is a radiating system. For both (the upper-resonance and lower-resonance) vortices in a patch resonator shown in Fig. 8 we have the same static magnetic field. This presumes the same direction of spin precession and so the same direction of time. There are, however, different directions of the Poynting-vector rotation for two coalescent resonance modes. It means that these resonant modes have different

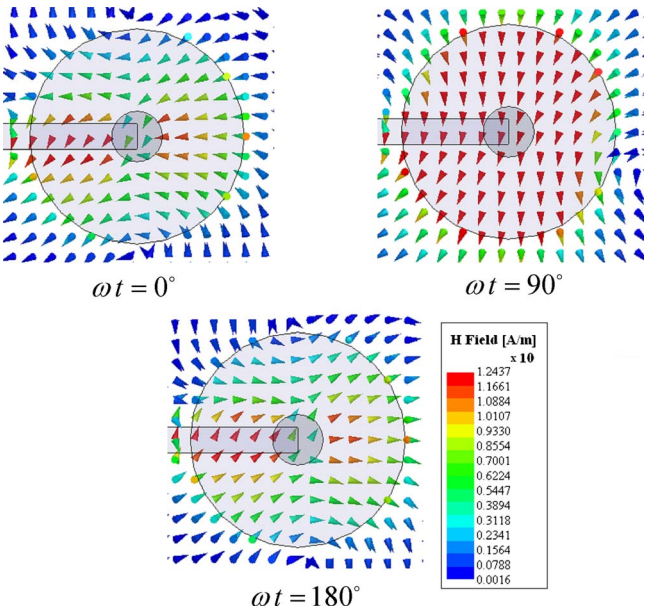

FIG. 13. (Color online) The magnetic field structure at different time phases inside a patch resonator with a ferrite disk at the lower-resonance frequency $f=2.72$ GHz (top view).

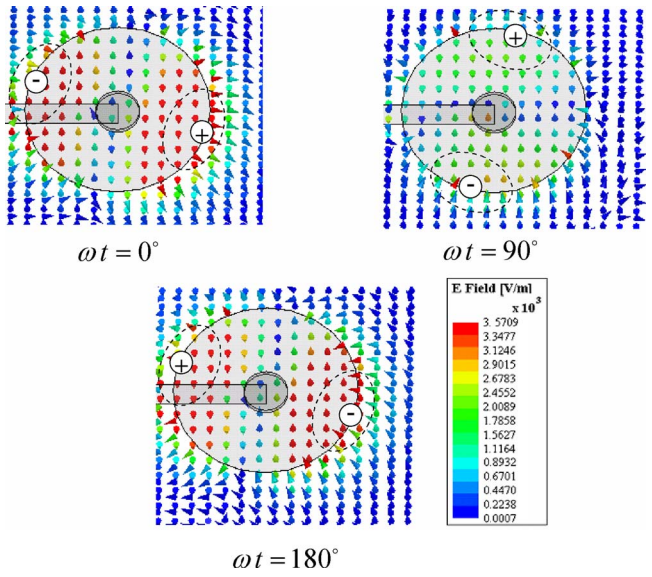

FIG. 14. (Color online) The electric field structure at different time phases inside a patch resonator with a ferrite disk at the lower-resonance frequency $f=2.72$ GHz (perspective view). There is a counterclockwise rotating electric dipole which appears due to electric charges on an edge of a patch.

chiralities: the left-hand chirality (with respect to the positive direction of z axis) for the upper resonance and the right-hand chirality for the lower resonance. We can call the upper resonance as the left-hand (LH) resonance of the doublet, while the lower resonance as the right-hand (RH) resonance of the doublet. The fact that for the observed two resonances there are different directions of the magnetic field rotation with respect to the same direction of the magnetization precession gives clear evidence for two different energies corresponding to these resonances. Contrary to experiments in Refs. 8 and 21, where the positive direction of time was given by the decay of the eigenstates in a dissipative system, in the present numerical experiment we discovered chiral states for the ferrite-induced topological singularities with the positive direction of time given by the direction of magnetization precession.

We observe distinctive chiral states as two different energy states in an open resonator. A geometric phase appears due to the nonzero circulation around the line where the wave function vanishes. In a TE polarized patch resonator, a circulation along the lines in space which surround a ferrite disk is described by Eq. (7) and can be represented as a circulation of a certain current-density-like quantity $\vec{j}$. From Figs. 9 and 12 it is evident that for the left-hand chiral state a ferrite disk behaves as a topological defect with a negative topological charge, while for the right-hand chiral state a ferrite disk behaves as a topological defect with a positive topological charge. The electric field distributions shown in Figs. 11 and 14 can be considered as the basis states $|1\rangle$ and $|2\rangle$ of two coalescent modes of the resonator. For the clockwise and counterclockwise rotations of these states (for the positive direction of time given by the direction of magnetization precession), a doublet is expressed as $|1\rangle+i|2\rangle$ similarly to Eq. (9).[8,21] The appearance of chiral phases in achiral system is one of the challenging problems in modern physics. We show that due to microwave-vortex topological de-

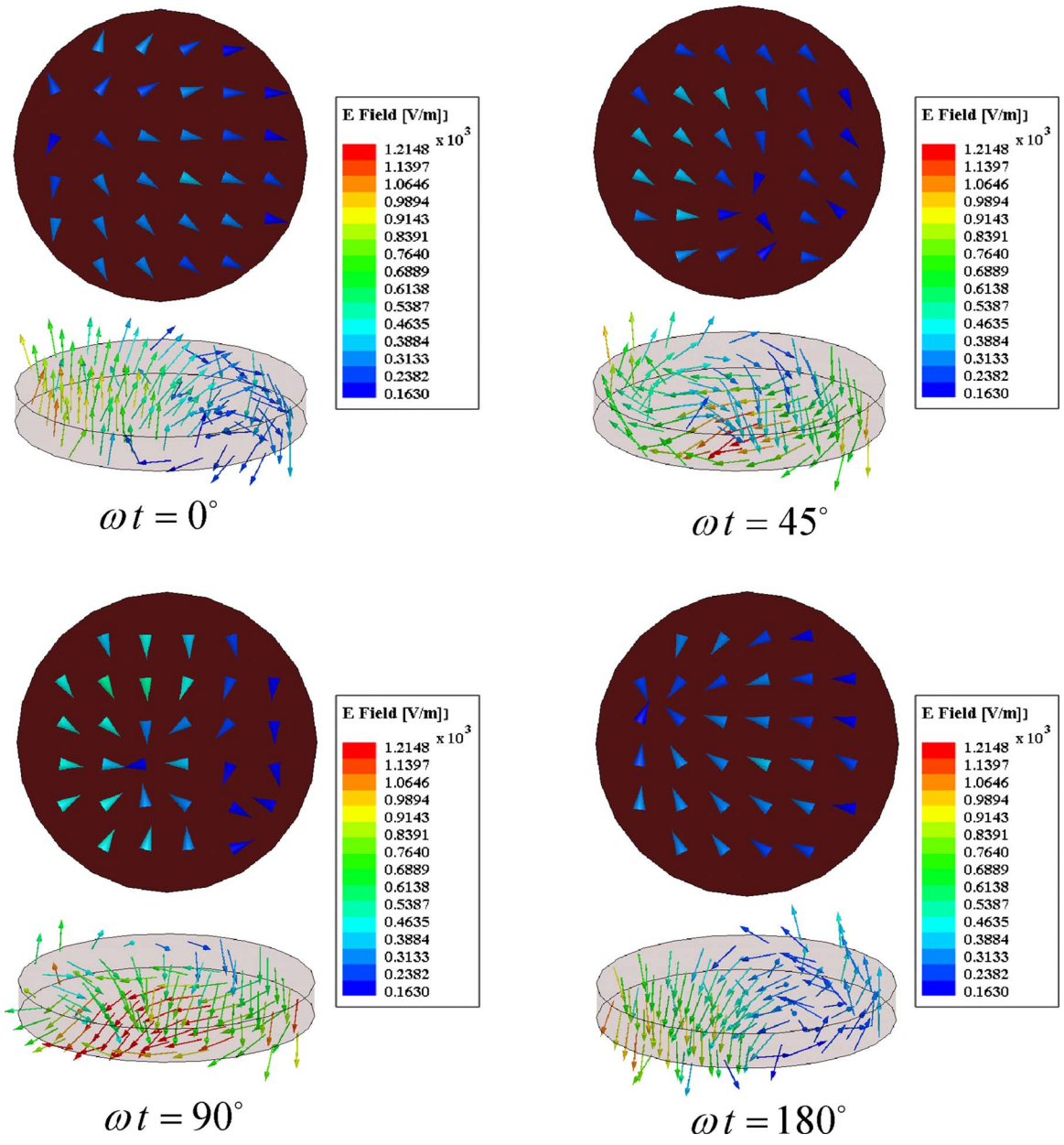

FIG. 15. (Color online) The top and perspective views of the electric field structure at different time phases inside a ferrite disk at the upper-resonance frequency $f=2.93$ GHz. An electric field inside a ferrite disk has a clockwise precession.

fects originated by small ferrite particles, magnetic gyrotropy can stipulate chirality in achiral electromagnetic structures. For the time invariance (because of a given direction of a bias magnetic field), one has clear discrimination of the chiral states [see Fig. 1(a)].

For further understanding physics of the observed chiral states, a deeper analysis of the fields inside a ferrite disk is required. In Sec. II of the paper we discussed that the effect of the electromagnetic field chiral rotation in media can be described by the gyration vector and the effective permeability tensor. Following our recent results in Ref. 5, inside a ferrite disk with the microwave vortex there is not only the magnetization precession, but also the precessing behavior of the electric-dipole polarization. In Figs. 15 and 16, we give the top and perspective views of the electric fields inside a ferrite disk for the upper-resonance and lower-resonance states at the same time phases. One can notice that for different resonant states, the directions of the electric field precession inside a ferrite are different. This effect of the electric field precession inside a ferrite disk underlies the physical mechanism of the observed chiral vortices in a patch resonator.

V. NEAR-FIELD CHIRAL VORTICES AND A FAR-FIELD SIGNATURE OF THE VORTEX CHIRAL STATES

The vortex chiral states originated from ferrite-disk topological defects become evident also in the radiating field structures of the patch. It is well known from Maxwell's theory that electromagnetic radiation carries both energy and momentum.[23] The momentum may have both linear and angular contributions. In free space, the angular momentum density is calculated as

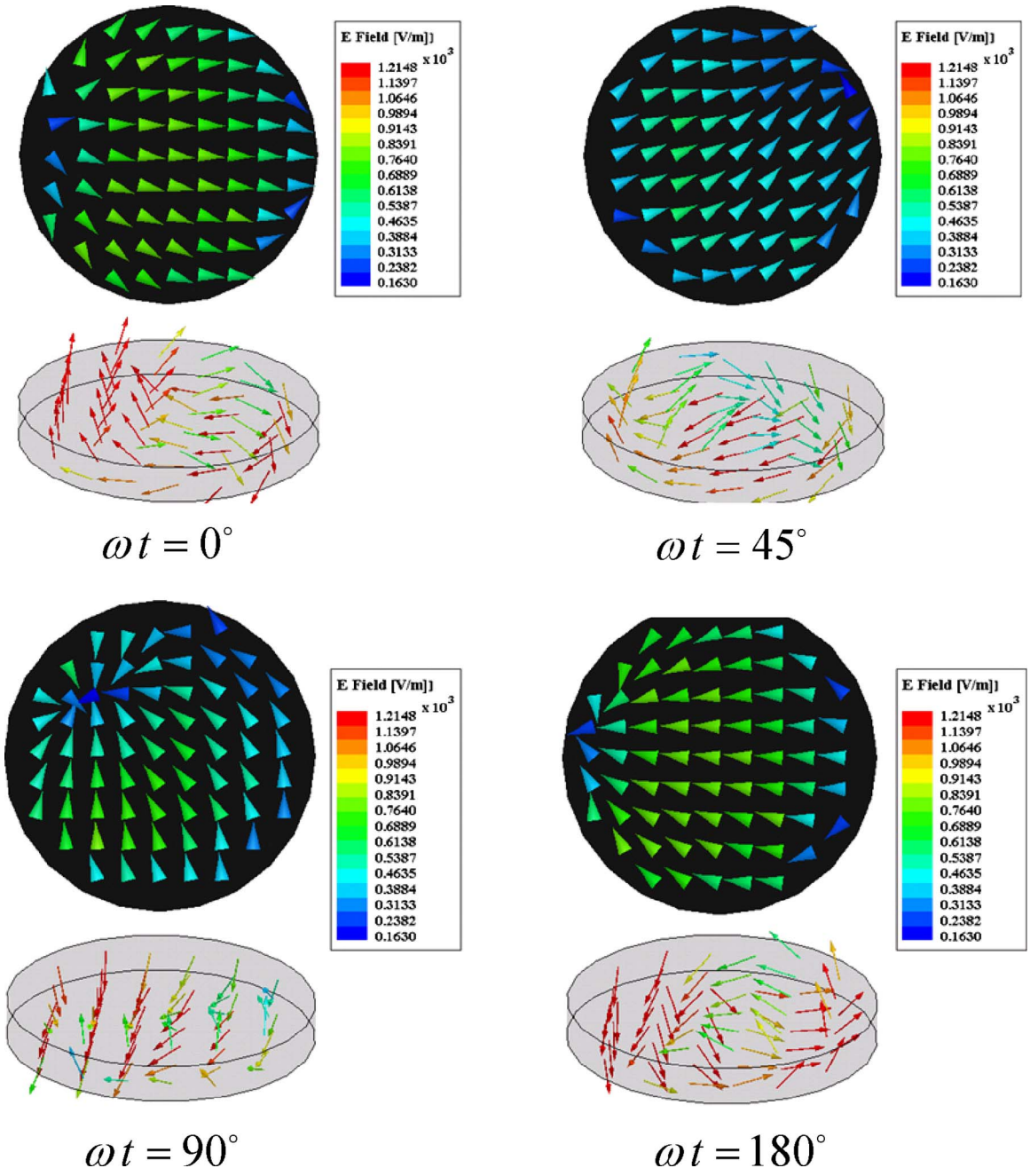

FIG. 16. (Color online) The top and perspective views of the electric field structure at different time phases inside a ferrite disk at the lower-resonance frequency $f=2.72$ GHz. An electric field inside a ferrite disk has a counter clockwise precession.

$$\vec{\mathcal{J}} = \frac{1}{4\pi c}\vec{r} \times (\vec{E} \times \vec{B}) \tag{9}$$

and is related in a simple way to the Poynting vector as

$$\vec{\mathcal{J}} = \frac{1}{c^2}\vec{r} \times \vec{S}. \tag{10}$$

In its turn, an angular momentum has a "spin" part associated with the field circular polarization in a given point and an "orbital" part associated with the spatial distribution of the linear momentum.[23] Only the total angular momentum, containing spin and orbital contributions, is a physical observable. In optical beams with a phase singularity on an axis, the orbital state rotates around the beam axis, whereas the spin state rotates around every given point.[24] This clearly corresponds to a mathematical concept of vorticity used in fluid dynamics. Recent interest in angular momentums of light beams has led to intensive studies of Laguerre-Gaussian beams which have helical wave fronts. On the other hand, correlation between an angular momentum of radiation and the Poynting-vector vortex structures was found in an electromagnetic field analysis of a rotating electric dipole.[25]

The vortex chiral states observed in a dielectric plate of a patch resonator with an enclosed ferrite disk are characterized by oppositely rotating electric dipoles which appear due to electric charges on the edge of the patch (see Figs. 11 and 14). The fields above the patch can be considered as originated from electric dipoles rotating above the ground plane.

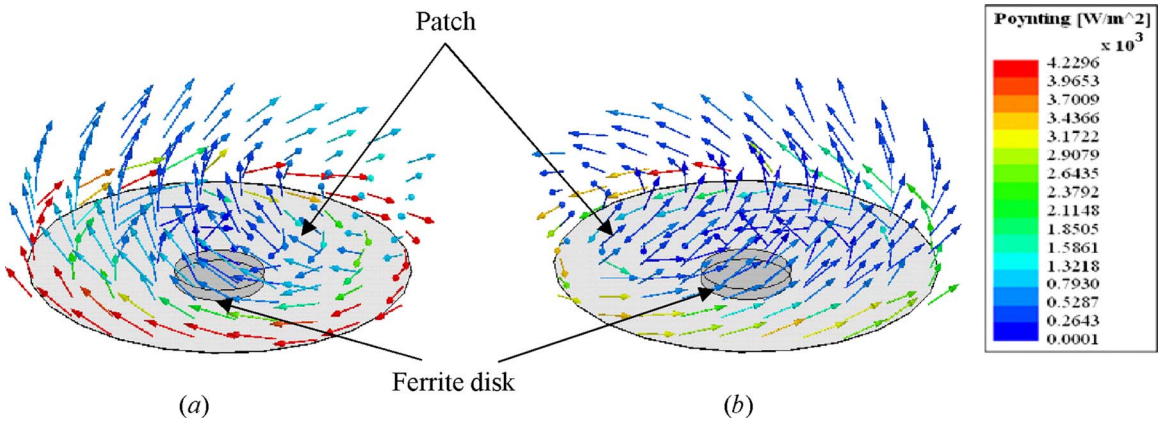

FIG. 17. (Color online) The Poynting vector distribution above the patch: (a) left-hand chiral state (f=2.93 GHz); (b) right-hand chiral state (f =2.72 GHz).

There are the left-handed circular polarized (LHCP) fields originated from the clockwise rotating electric dipole shown in Fig. 11 and the right-handed circular polarized (RHCP) fields originated from the counterclockwise rotating electric dipole shown in Fig. 14. In the near-field region, the lines of the Poynting vector circulate around the z axis with the same direction as the rotation of the electric dipole moment (see Fig. 17). The space-time evolution of a wave is governed by its phase front topology. In vacuum, the Poynting vector has the same direction as a linear momentum of the field. The radiating fields of two coalescent chiral modes have the left-handed and right-handed helical wave fronts. In a certain near-field cross-sectional (perpendicular to z axis) region above a patch one has a correlation between the direction of

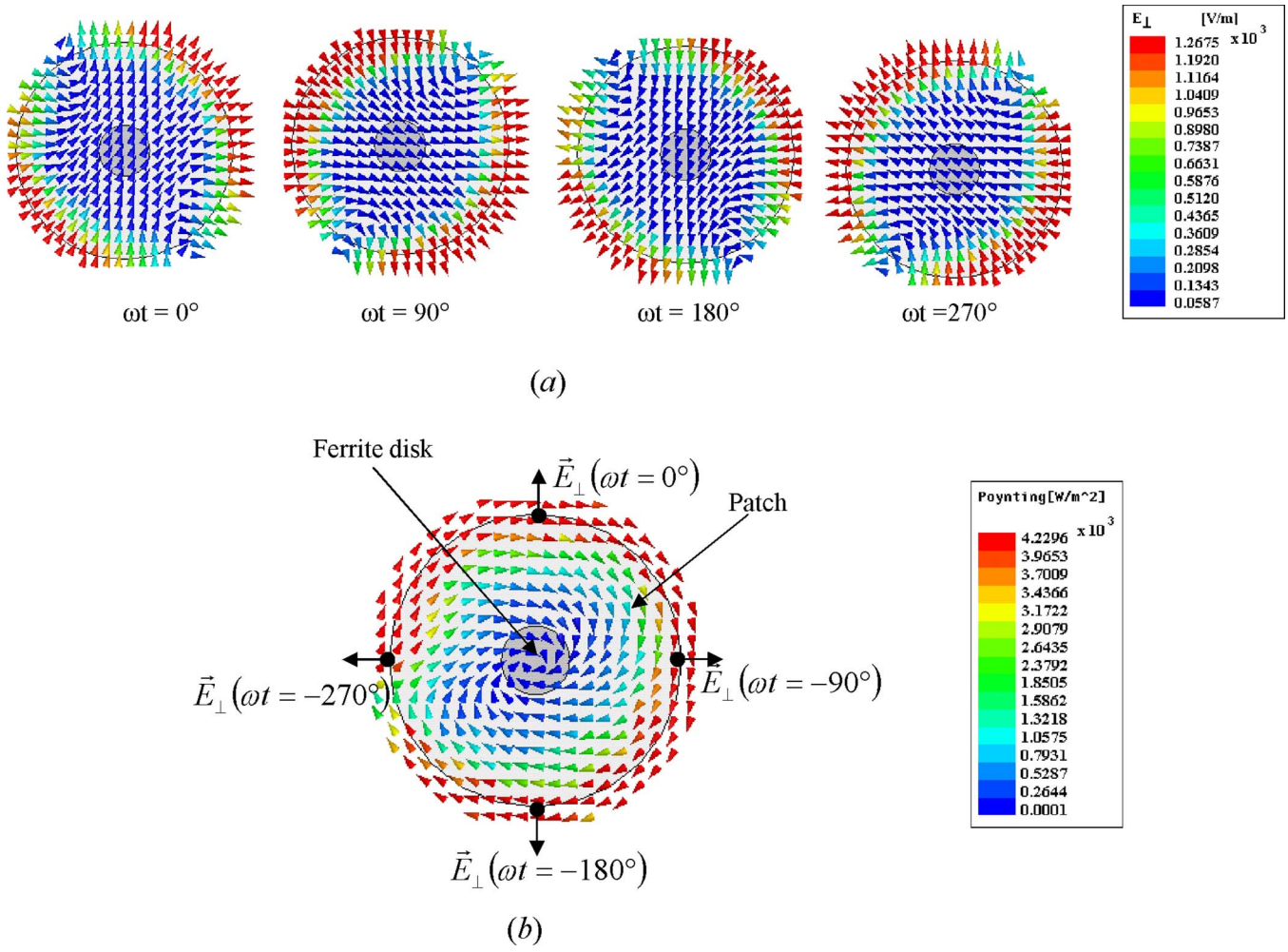

FIG. 18. (Color online) Evidence for the field vortex structure above the patch for the left-hand chiral state (f=2.93 GHz). (a) The transverse electric field has the LH circular polarization in every point; (b) the transverse component of Poynting vector associated with the electric field distribution.

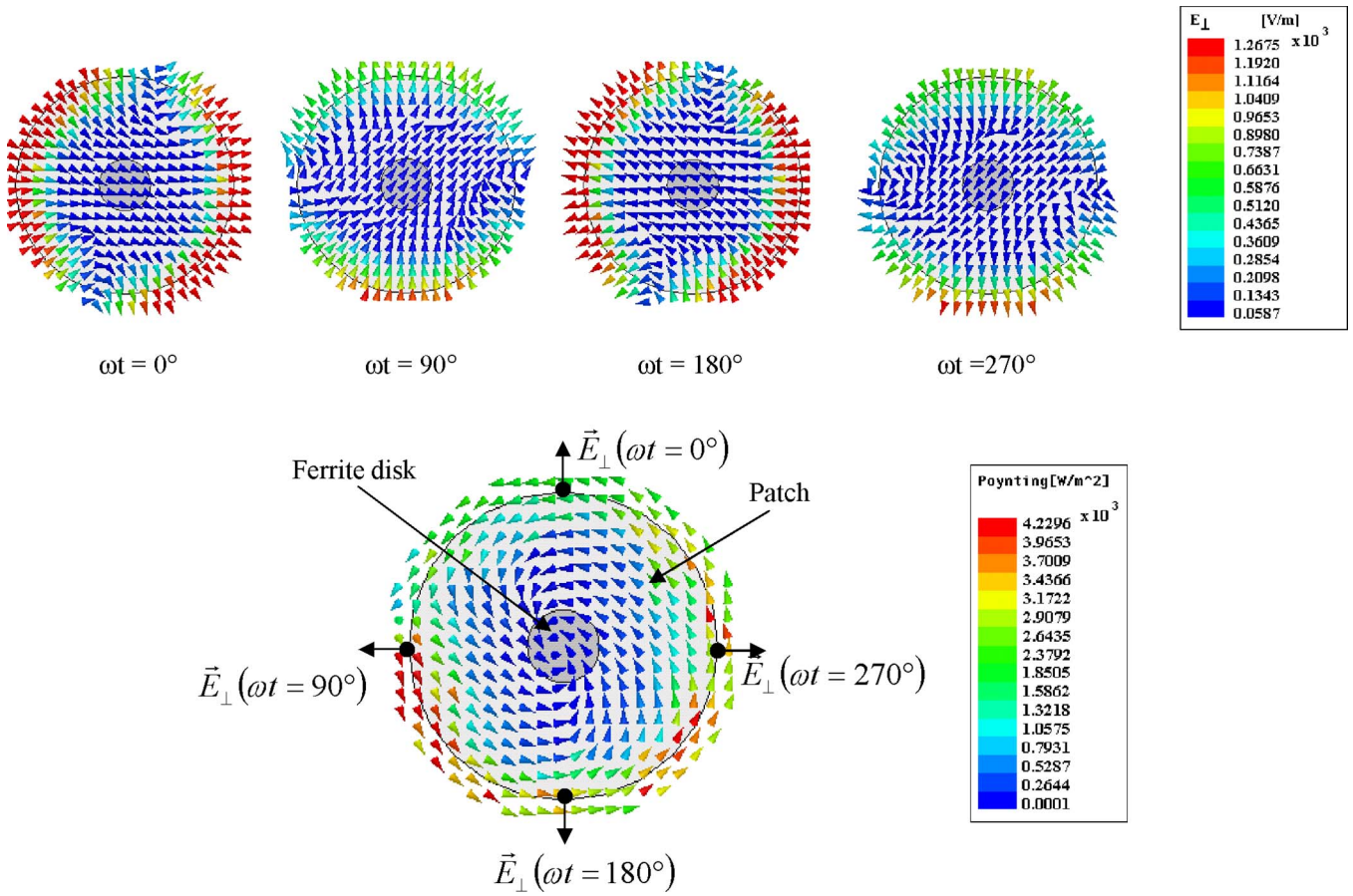

FIG. 19. (Color online) Evidence for the field vortex structure above the patch for the right-hand chiral state (f=2.72 GHz). (a) The transverse electric field has RH circular polarization in every point; (b) the transverse component of Poynting vector associated with the electric field distribution.

the Poynting vector (linear momentum) rotation and a direction of a field polarization rotation. Figures 18 and 19 give evidence of the field vortex structures above the patch at a cross-sectional [for certain $z>0$; see Fig. 7(b)] region for the left-hand and right-hand chiral states, respectively. One can see the transverse electric field circular polarization and the transverse component of Poynting vector (linear momentum) associated with the electric field distribution. There is an orbital momentum rotation around the axis directed along the normal of the ferrite disk together with the field spin rotation.

In the far-field region there are no vortices. Nevertheless, as a signature of the vortex chiral states inside the patch resonator and in a near-field region, one can distinguish the polarization chiral states of electromagnetic fields in a far-field region. To characterize the field polarization properties of the far-field radiation we analyze the axial ratio. The axial ratio is defined as the ratio of the major to minor axes of the polarization ellipse. Figure 20 shows the frequency dependence of the axial ratio. One can see that at frequencies corresponding to the left-hand (f=2.93 GHz) and right-hand (f=2.72 GHz) resonances there are minimums of the axial ratio. The effectiveness of the radiation field pattern is characterized by a parameter of directivity. The directivity is equal to the ratio of the maximum power density in polar coordinates $P(\theta,\varphi)_{\max}$ to its average value over a sphere surrounding the antenna.[22] One can define the directivities for the LHCP and RHCP radiation fields. Figure 21 shows the frequency dependency of the directivities for two types of circularly polarized radiations. It is evident that a maximal directivity for the left-hand circularly polarized radiation is at frequency f=2.93 GHz, while for the right-hand circularly polarized radiation one has a maximal gain at frequency f=2.72 GHz. So there is clear correspondence between the near-field chiral topology and the far-field polarization structure. The observed LHCP and RHCP far-field polarization structures represent a doublet of chiral vortices in space originated from a doublet of resonant chiral states in the patch.

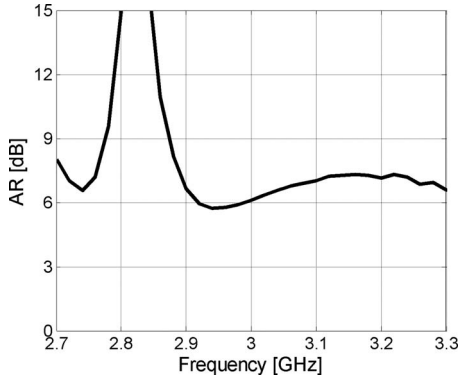

FIG. 20. An axial ratio for the far-field structure of a patch resonator with a ferrite disk.

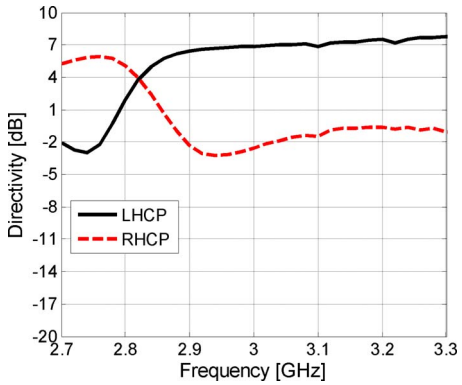

FIG. 21. (Color online) Directivities for the RHCP and LHCP far-field structures of a patch resonator with a ferrite disk.

VI. CONCLUSION AND DISCUSSION

Based on numerical experiments, we have shown that in open resonant microwave structures with ferrite inclusions there exist vortex-type fields and Poynting-vector phase singularities. In such structures one can observe a pair of resonances which have different directions of the vortex rotation at the same direction of time. Such ferrite-induced topological singularities are chiral states. There is a clear difference between the effects of chirality and magnetic gyrotropy. In a case of chirality one has time-invariant states with parity nonconservation, while in a case of magnetic gyrotropy one has parity conservation with the TRS breaking. To be able to discriminate the states with different chirality in dynamical systems one should be able to realize a situation with a concrete direction of time. Contrary to the chirality characterization in a dissipative microwave resonator via the direction of time given by the decay process,[8] in the present numerical experiment we characterize the chiral states via the direction of time given by the direction of the magnetization precession. The observed chiralities in a patch resonator with an enclosed ferrite disk are strongly correlated with the type of the radiating fields: for the LH chirality one has the LHCP radiating field and for the RH chirality one has the RHCP radiating field.

A structure of the considered patch resonator with an enclosed ferrite disk resembles, to a certain extent, a cylindrical resonator with ferrites used for so-called Y-circulators.[3] The circulator devices, however, have nothing in common with the observed chiral-state behaviors. For a given direction of the normal dc magnetic field, in Y-circulators one has a certain azimuth distribution of the field amplitudes at frequency $\omega_- < \omega_0 < \omega_+$, where ω_- and ω_+ are the frequencies of the counterclockwise and clockwise field rotations. The circulator works due to the *standing* wave behavior giving the azimuth distribution of energy in microwave ports. The opposite circularity of the standing wave energy can be obtained when one reverse a direction of the dc magnetic field. There are no azimuthally running power flows leading to the vortex creation.

Vortices are topological defects which appear due to dynamical symmetry breaking. While electromagnetic scattering from chiral objects is a well known problem,[10,11] there are no effects originated from the chiral-state topological defects. Following our results, one comes to a rather unexpected and interesting conclusion: a circularly polarized EM radiation obtained from a chiral-state vortex antenna with a small ferrite inclusion can be considered as being originated from a vortex topological defect in space. Two coalescent resonances are the states with chiral symmetry.

[1] M. S. Soskin, V. N. Gorshkov, M. V. Vasnetsov, J. T. Malos, and N. R. Heckenberg, Phys. Rev. A **56**, 4064 (1997); I. Bialynicki-Birula and Z. Bialynicki-Birula, *ibid.* **67**, 062114 (2003); J. Leach, M. R. Dennis, J. Courtial, and M. J. Padgett, N. J. Phys. **7**, 55 (2005).
[2] P. So, S. M. Anlage, E. Ott, and R. N. Oerter, Phys. Rev. Lett. **74**, 2662 (1995); M. Vraničar, M. Barth, G. Veble, M. Robnik, and H.-J. Stockmann, J. Phys. A **35**, 4929 (2002); M. Barth and H.-J. Stöckmann, Phys. Rev. E **65**, 066208 (2002); H. Schanze, H.-J. Stockmann, M. Martinez-Mares, and C. H. Lewenkopf, , *ibid.* **71**, 016223 (2005).
[3] A. G. Gurevich and G. A. Melkov, *Magnetic Oscillations and Waves* (CRC Press, New York, 1996).
[4] E. O. Kamenetskii, M. Sigalov, and R. Shavit, Phys. Rev. E **74**, 036620 (2006).
[5] M. Sigalov, E. O. Kamenetskii, and R. Shavit, Phys. Lett. A **372**, 91 (2008).
[6] M. Sigalov, E. O. Kamenetskii, and R. Shavit, J. Appl. Phys. **103**, 013904 (2008).
[7] B. Dietz, T. Friedrich, H. L. Harney, M. Miski-Oglu, A. Richter, F. Schafer, and H. A. Weidenmuller, Phys. Rev. Lett. **98**, 074103 (2007).
[8] C. Dembowski, H.-D. Gräf, H. L. Harney, A. Heine, W. D. Heiss, H. Rehfeld, and A. Richter, Phys. Rev. Lett. **90**, 034101 (2003).
[9] H. F. Schouten, T. D. Visser, G. Gbur, and D. Lenstra, Phys. Rev. Lett. **93**, 173901 (2004).
[10] A. Papakostas, A. Potts, D. M. Bagnall, S. L. Prosvirnin, H. J. Coles, and N. I. Zheludev, Phys. Rev. Lett. **90**, 107404 (2003).
[11] B. Bai, Y. Svirko, J. Turunen, and T. Vallius, Phys. Rev. A **76**, 023811 (2007).
[12] L. D. Landau and E. M. Lifshitz, *Electrodynamics of Continuous Media*, 2nd ed. (Pergamon, Oxford, 1984).
[13] A. Yariv and P. Yeh, *Optical Waves in Crystals* (Wiley, New York, 1983).
[14] I. V. Lindell, A. H. Sihvola, S. A. Tretyakov, and A. J. Viitanen, *Electromagnetic Waves in Chiral and Bi-Isotropic Media* (Artech House, Boston, 1994).
[15] R. E. Raab and O. L. De Lange, *Multipole Theory in Electromagnetism* (Clarendon, Oxford, 2005).
[16] E. O. Kamenetskii, Phys. Rev. E **58**, 7965 (1998).
[17] L. D. Baron, *Molecular Light Scattering and Optical Activity* (Cambridge University, Cambridge, 1982).
[18] A. L. Shelankov and G. E. Pikus, Phys. Rev. B **46**, 3326 (1992).
[19] S. S. Gupta and N. C. Srivastava, Phys. Rev. B **19**, 5403 (1979); A. S. Akyol and L.E. Davis, European Microwave Conference, London, 2001, Vol. 1, pp.229–232, and Vol. 31.
[20] W. Wang and M. Takeda, Phys. Rev. Lett. **96**, 223904 (2006).
[21] C. Dembowski, B. Dietz, H.-D. Gräf, H.-L. Harney, A. Heine, W. D. Heiss, and A. Richter, Phys. Rev. E **69**, 056216 (2004).
[22] C. Balanis, *Antenna Theory: Analysis and Design*, 2nd ed. (Wiley, New York, 1997).
[23] J. D. Jackson, *Classical Electrodynamics*, 2nd ed. (Wiley, New York, 1975).
[24] L. Allen, M. W. Beijersbergen, R. J. C. Spreeuw, and J. P. Woerdman, Phys. Rev. A **45**, 8185 (1992).
[25] H. F. Arnoldus and J. T. Foley, Opt. Commun. **231**, 115 (2004).